

Monsoon hydrography and productivity changes in the East China Sea during the past 100,000 years: Okinawa Trough evidence (MD012404)

Yuan-Pin Chang,^{1,2} Min-Te Chen,¹ Yusuke Yokoyama,^{3,4,5} Hiroyuki Matsuzaki,⁶ William G. Thompson,⁷ Shuh-Ji Kao,⁸ and Hodaka Kawahata³

Received 25 November 2007; revised 16 May 2009; accepted 23 June 2009; published 29 August 2009.

[1] We analyzed the high-resolution foraminifer isotope records, total organic carbon (TOC), and opal content from an Okinawa Trough core MD012404 in order to estimate the monsoon hydrography and productivity changes in the East China Sea (ECS) of the tropical western Pacific over the past 100,000 years. The variability shown in the records on orbital time scales indicates that high TOC intervals coincide with the increases of boreal May–September insolation driven by precession cycles (~21 ka), implying a strong connection to the variations in monsoons. We also observed possibly nearly synchronous, millennial-scale changes of the ECS surface hydrography (mainly driven by salinity changes but also by temperature effects) and productivity coincident with monsoon events in the Hulu/Dongge stalagmite isotope records. We found that increased freshening and high productivity correlate with high monsoon intensity in interstadials. This study suggests that the millennial-scale changes in monsoon hydrography and productivity in the ECS are remarkable and persistent features over the past 100,000 years.

Citation: Chang, Y.-P., M.-T. Chen, Y. Yokoyama, H. Matsuzaki, W. G. Thompson, S.-J. Kao, and H. Kawahata (2009), Monsoon hydrography and productivity changes in the East China Sea during the past 100,000 years: Okinawa Trough evidence (MD012404), *Paleoceanography*, 24, PA3208, doi:10.1029/2007PA001577.

1. Introduction

[2] Monsoons play an important role in the latitudinal transfer of heat and moisture between the tropics and high latitudes. Monsoon circulations in East Asia are characterized by continental heating, the development of low pressure on the continent, and moderate-strength southwest winds which bring heat and moisture from the seas to the interior of the continent in the summer. This seasonally reversing wind strongly impacts the regional surface and subsurface ocean circulation, which in turn changes the composition of the underlying sediments, providing a means of monitoring past variability in the monsoon system. The monsoon impacts of ocean circulation as well as sediment core composition changes at geological time scales have been investigated intensively in the Arabian Sea

[Clemens *et al.*, 1991, 2003] and in the South China Sea and Sulu Sea [Chen and Huang, 1998; Wang *et al.*, 1999b, 1999a; Oppo *et al.*, 2003; Yu *et al.*, 2006]. On orbital time scales, changes of precession (~21 ka cycles) modulate the seasonal distribution of incoming solar insolation, thus the precession variation has long been recognized as a primary forcing of the monsoon changes [Kutzbach and Guetter, 1986; Prell and Kutzbach, 1987].

[3] Recent paleoclimate data [Wang *et al.*, 2001; Yuan *et al.*, 2004; Cheng *et al.*, 2006; Partin *et al.*, 2007; Wang *et al.*, 2008] that have been reconstructed from land-based stalagmite records suggest that the monsoon system in the tropical western Pacific might play an important role in more abrupt, millennial-scale climate changes. Heavy summer monsoon precipitation that discharges enormous amounts of fresh water and sediments into the marginal seas of the tropical western Pacific is considered to be one of the important components of global hydrological cycles. The perturbations of the hydrological cycles may have an impact on thermohaline circulation [Schmittner and Clement, 2002], an important climate component for driving millennial-scale changes. Ocean records of monsoon variability on the scale of millennia are sporadic [Dannenmann *et al.*, 2003; Oppo *et al.*, 2003; Oppo and Sun, 2005] or short in time length [Wang *et al.*, 1999b, 1999a], and thus are not sufficient to determine more regional patterns that could be compared with results from modeling studies [Bush and Philander, 1999; Bush and Fairbanks, 2003; Zhang and Delworth, 2005]. Additional high-resolution records that cover more temporal and spatial scales are therefore needed.

¹Institute of Applied Geosciences, National Taiwan Ocean University, Keelung, Taiwan.

²Now at Institute of Marine Geology and Chemistry, National Sun Yat-sen University, Kaohsiung, Taiwan.

³Ocean Research Institute, University of Tokyo, Tokyo, Japan.

⁴Department of Earth and Planetary Sciences, University of Tokyo, Tokyo, Japan.

⁵Institute of Biogeosciences, Japan Agency for Marine-Earth Science and Technology, Yokosuka, Japan.

⁶Department of Nuclear Engineering and Management, University of Tokyo, Tokyo, Japan.

⁷Department of Geology and Geophysics, Woods Hole Oceanographic Institution, Woods Hole, Massachusetts, USA.

⁸Research Center for Environmental Changes, Academia Sinica, Taipei, Taiwan.

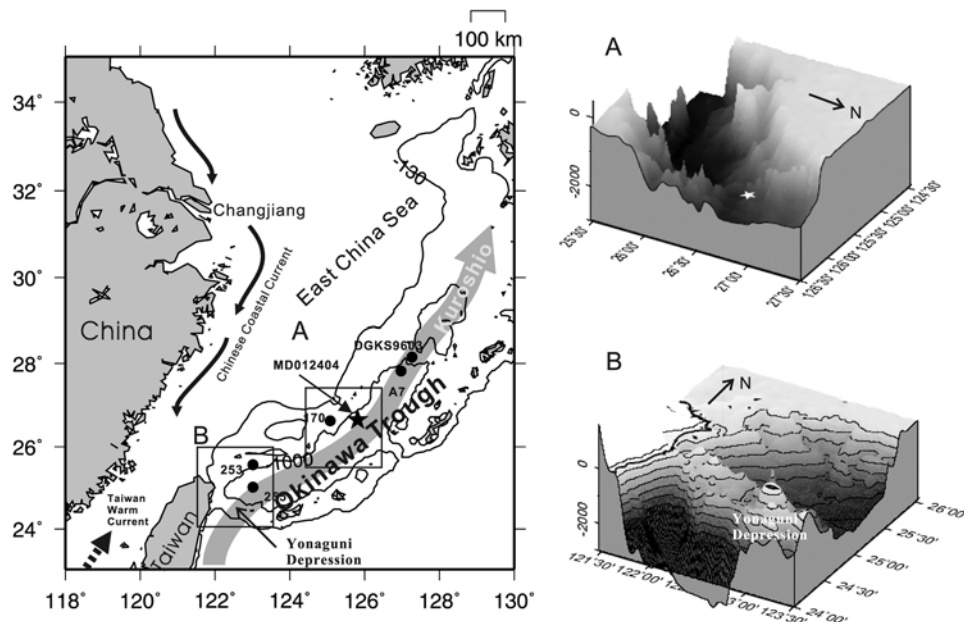


Figure 1. Maps showing the location and regional topography of core MD012404 in the Okinawa Trough (OT) and East China Sea (ECS). The flow path of the Kuroshio is indicated by a gray line. Locations of cores we previously studied are shown: 253 [Li et al., 1997], 255 [Li et al., 1997; Jian et al., 2000], 170 [Li et al., 1997], A7 [Sun et al., 2005; Xiang et al., 2007], and DGKS9603 [Li et al., 2001]. Submarine topography A showing that the coring site is located in a small topographic low near the western edge of the OT and submarine topography B near an offshore area of northeastern Taiwan showing the sills near Ryukyu Island or the Yonaguni Depression (water depth ranges from 300 to 600 m).

[4] In order to better evaluate the timing of East Asian summer monsoon variations of orbital to millennial scales and their hydrographic impact on surrounding seas, we present here a high-resolution study based on a marine sedimentary core (MD012404) retrieved in an IMAGES program cruise from the central Okinawa Trough (OT), in the East China Sea (ECS) (Figure 1). We have measured planktic and benthic foraminifer oxygen isotopes as proxies for estimating regional sea surface hydrography (mainly for salinity, SSS and temperature, SST), and used benthic isotope stratigraphy and planktic foraminifer AMS ^{14}C dating to establish high-precision age controls. We also used various biogenic components such as total organic carbon (TOC) and opal content as proxies for productivity in the ECS over the past $\sim 100,000$ years. The preliminary oxygen isotope age model and TOC data have been presented in previous studies [Chang et al., 2005, 2008]. On the basis of these initial results, the core is characterized by a high sedimentation rate ($\sim 50 \text{ cm ka}^{-1}$) that permits observation of not only orbital-scale variations, but also millennial-scale.

[5] The geographic setting of the ECS and OT regions is such that winter and summer monsoon circulations dominate the seasonal patterns of SST and SSS (Figure 2), winds, precipitation, and runoff over East Asia. The ECS is located off the east coast of the Asian continent that extends around 1300 km from 24°N to 32°N ; it occupies more than $800,000 \text{ km}^2$ and is one of the biggest marginal seas in the world. The Changjiang (Yangtze River), one of the

largest rivers on the planet, discharges an annual mean of $\sim 3.0 \times 10^4 \text{ m}^3 \text{ s}^{-1}$, which accounts for almost 90% of the whole river discharge into the ECS [Beardsley et al., 1985]. Most of the deposited sediments in the ECS shelves are also received from the Changjiang, and the output is greater than $\sim 5 \times 10^8 \text{ t}$ every year [Milliman and Meade, 1983]. The OT is a tectonically active back-arc-spreading basin extended in a northeast-southwest direction between the ECS shelf and the Ryukyu arc. The opening history of the OT can be dated back to the middle Miocene [Sibuet et al., 1998]. Since that time, the OT has been a depositional center in the ECS and has received a large sediment supply from nearby rivers. The main ocean current affecting the OT is the Kuroshio, which flows northward along the eastern coast of Taiwan, with a maximum speed of 100 cm s^{-1} and a width of 100 km [Liang et al., 2003]. The north-eastward flowing Kuroshio follows the curved isobaths and leaves the ECS through the Tokara Strait, south of Kyushu, Japan. The modern flow patterns of the Kuroshio are controlled by the bathymetry of the OT. A northern branch current, the Tsushima Current, flows into the Japan Sea and is affected by the shallow sill depth ($\sim 130 \text{ m}$) in the Tsushima Strait. In the south, the intrusion flows into the southern OT that is affected by the sills near Ryukyu Island or the Yonaguni Depression (with water depths ranging from 300 to 600 m) (Figure 1). Shelfward intrusion of the Kuroshio is also responsible for inducing cyclonic eddies [Hsu et al., 1998; Tang et al., 2000; Liang et al., 2003],

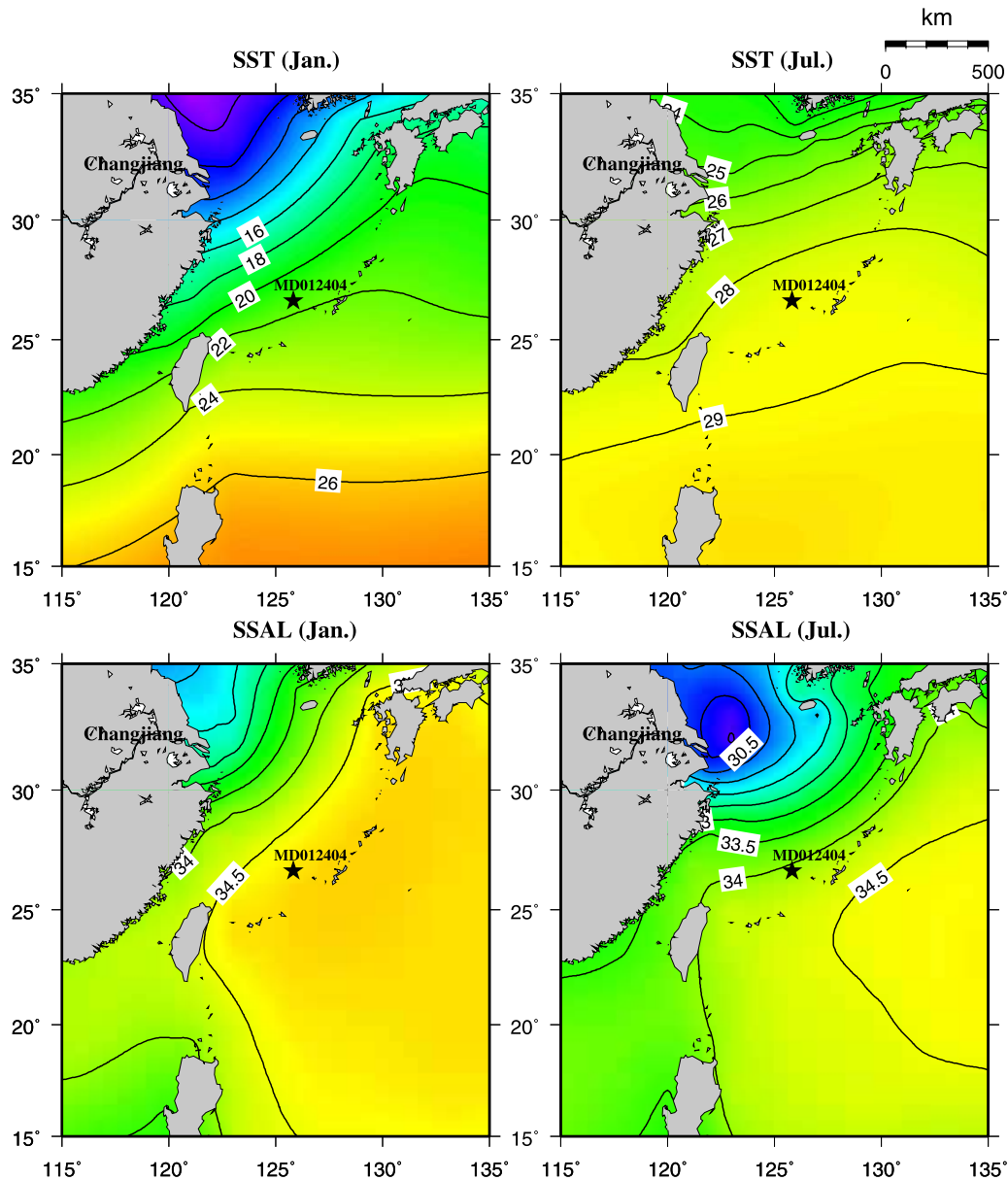


Figure 2. Distributions of modern sea surface temperature (SST) and sea surface salinity (SSS) during January and July. In the summer, more freshwater outflows into the East China Sea are from the Changjiang and the Yellow River. The data are based on the 1994 World Ocean Atlas (WOA) [Levitus and Boyer, 1994].

which represent efficient gateways for cross-shelf transfer of nutrients and suspended sediments into the deep ECS.

[6] By examining paleoceanographic proxies from sediment cores from the ECS and OT, long-term observational studies such as that presented here can provide independent insight into the past dynamics of monsoon precipitation, surface water hydrography, and upwelling/productivity of orbital to millennial time scales in the tropical western Pacific. The main objectives of this study are to (1) reconstruct the long-term, millennia-scale surface hydrography and productivity changes of ~the past 100,000 years using foraminifer isotope and biogenic component variations in a sediment core retrieved from the OT; (2)

determine the timing of the intensity of the monsoon changes in the ECS on the basis of the marine hydrography and productivity records; and (3) evaluate the potential linkages of the monsoon hydrography and productivity variations to those shown in land-based stalagmite monsoon records, and to major global climate forcing factors such as orbital and ice volume/sea level variations.

2. Data and Methods

[7] Core MD012404 was taken during the year 2001 IMAGES program cruise at 26°38.84'N, 125°48.75'E, in the central OT. The water depth of the core is 1397 m, and

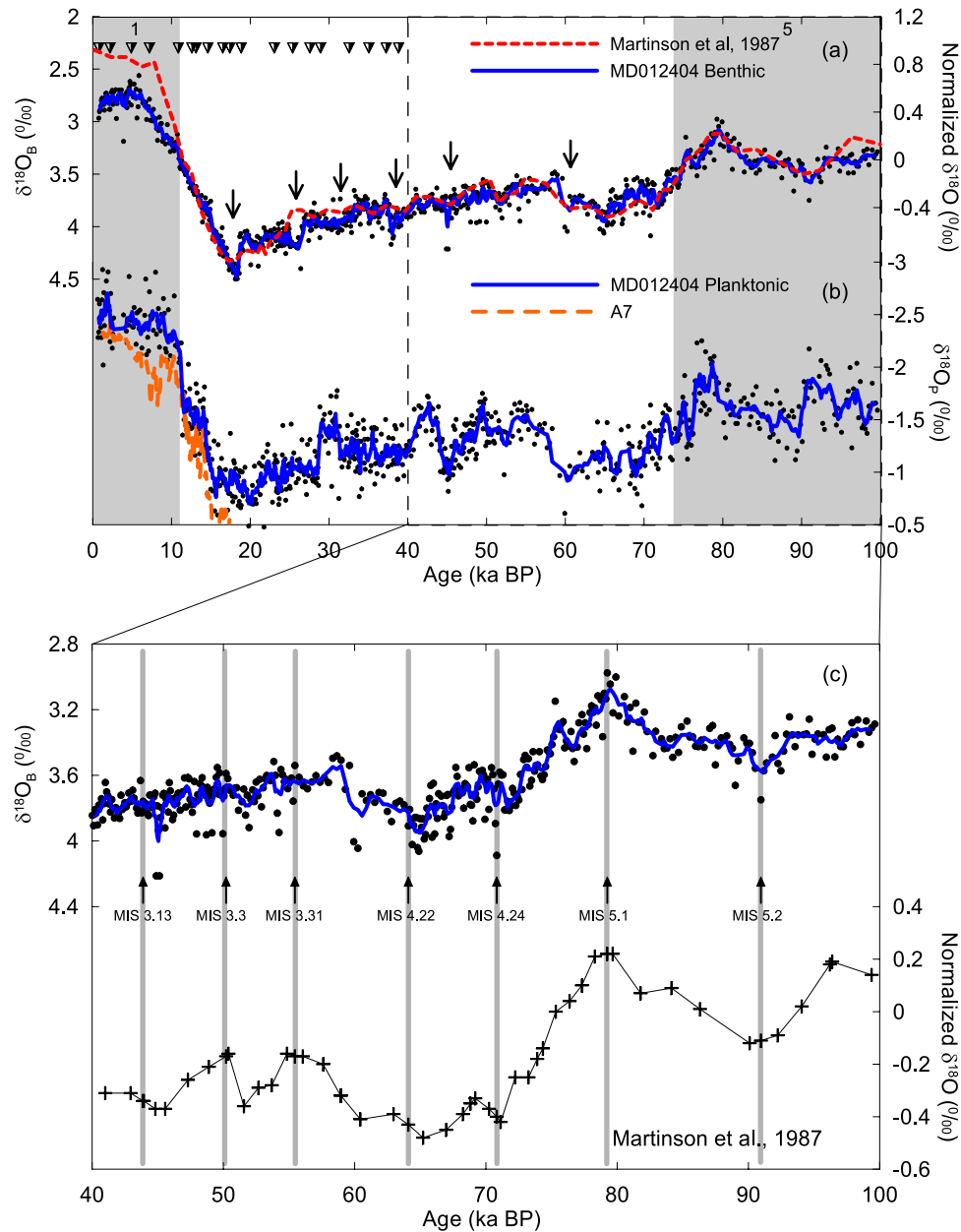


Figure 3. (a) Benthic and (b) planktic foraminifer $\delta^{18}\text{O}$ of core MD012404. Solid lines are five-point averaging lines from the original data points (shown as dots). Triangles indicate 19 AMS ^{14}C dating, and plain arrows indicate the isotope age control points that were used for developing the age model. Bold arrows on the top of the benthic $\delta^{18}\text{O}$ indicate short-lived heavy intervals occurring during the timing of Heinrich events in high latitudes [Bond *et al.*, 1992]. (c) A planktic foraminifer $\delta^{18}\text{O}$ (shown in blue) from nearby core A7 [Sun *et al.*, 2005] is plotted for comparison. An enlarged version of age control points chosen for MIS 3–5, with respect to a stack curve [Martinson *et al.*, 1987], is shown (bottom curve). Our age control points were chosen on the basis of the correlation between the MD012404 benthic isotope curve and the stack curve. The isotope age control points were adopted from a preliminary study [Chang *et al.*, 2005], and were determined from choosing the average depths of valley or peak structures shown in the isotope data, and then fine-tuned in order to reach a more stable sedimentation rate for the core.

the total length is 44 m [Bassinot *et al.*, 2002]. The coring site is located in a small topographic low near the western edge of the OT, which is ideal for trapping downward settling biogenic particles in the water column (Figure 1).

Sediments in this core are mainly composed of nearly homogenous nannofossil ooze or diatom-bearing nannofossil ooze. No visible turbidite or tephra layer was found in the core, but pumice and volcanic glass could be observed

under the microscope at some depths, perhaps implying the long-distance transport of volcanic materials via the atmosphere and/or the redeposition of the sediments from nearby continentals. Core samples are archived in the core repository and laboratory of the National Center for Ocean Research at Keelung, Taiwan (<http://corelab.iag.ntou.edu.tw>).

[8] Samples taken from the core at 10 cm intervals were analyzed for benthic (*Uvigerina* spp.) and planktic foraminifer (*Globigerinoides ruber* (white), sensu stricto

form, 250–300 μm) isotopes (Figure 3), and for their carbonate, TOC, and opal contents (Figure 4). Planktic foraminifer shells were cracked gently into fragments to remove extraneous materials before the isotope measurements, which were made with a Micromass IsoPrime isotope ratio mass spectrometer at the Geological Survey of Japan, National Institute of Advanced Industrial Science and Technology (AIST) at Tsukuba, Japan. An international standard (NBS-19) was used to calibrate the measured values to a Pee Dee belemnite (PDB) unit. Machine error based on the

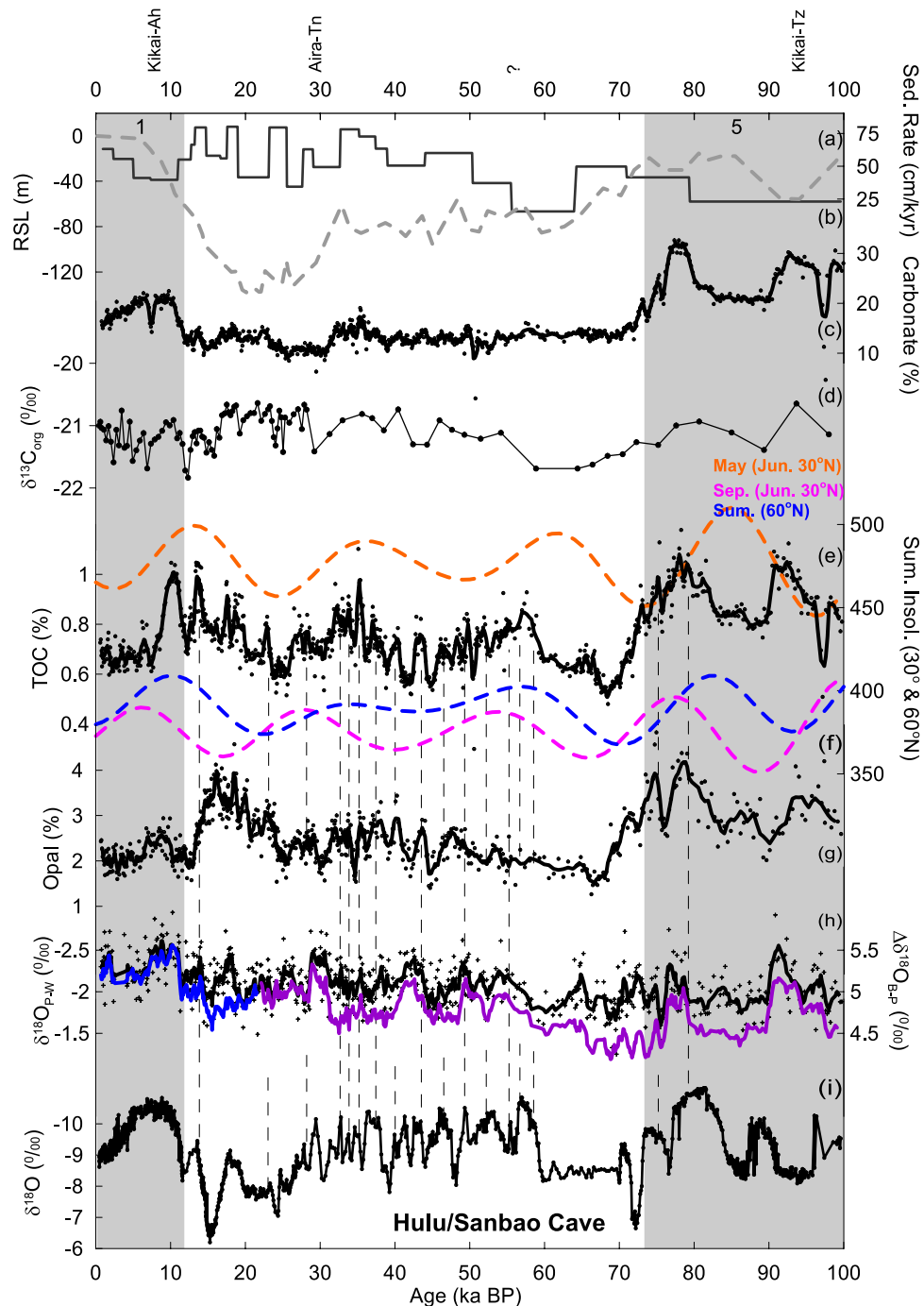


Figure 4

analyses of the standards was under 0.05‰ for the oxygen isotopes and less than 0.03‰ for the carbon isotopes.

[9] The carbonate and TOC data of the core and their experimental details have been presented by *Chang et al.* [2005]. We also measured the biogenic opal contents (SiO_2) in the samples. Approximately 0.2 g dry powder from each sample was weighed and transferred into a 50 ml polypropylene centrifuge tube. Carbonates and organic matter in the samples then were removed by hydrochloric acid (HCl) and peroxide (H_2O_2). 40 ml 2M Na_2CO_3 was added to the samples and then they were placed in a water bath and heated to 85°C. Dissolved silica in the extraction was measured by the molybdate blue spectrophotometric method with a Perkin Elmer Lambda Bio 20 spectrophotometer, and the silica contents were translated into opal content by a procedure presented by *Mortlock and Froelich* [1989]. The standard error was <0.1% in our repeated measurements.

[10] A preliminary age model of core MD012404 has been published previously [*Chang et al.*, 2005], but that age model was based only on 5 AMS ^{14}C dating and oxygen isotope age controls from a SPECMAP stack [*Imbrie et al.*, 1984]. In the current study, a new fine-tuned age model for this core was constructed for using 19 Accelerator Mass Spectrometry (AMS) ^{14}C ages of the last 40,000 years, and oxygen isotope age control points were determined from a correlation between the benthic isotope curve with a more high resolution stack curve [*Imbrie et al.*, 1984; *Pisias et al.*, 1984; *Martinson et al.*, 1987] (Table 1 and Figure 3). The AMS ^{14}C measurements were done by taking ~20 mg of the planktic foraminifers *G. ruber* and *G. sacculifer* (>250 μm), dated at the Micro Analysis Laboratory, Tandem Accelerator (MALT), the University of Tokyo. All AMS ^{14}C ages were adjusted for a mean Pacific reservoir age of 400 years, and then calibrated according to *Fairbanks et al.* [2005]. We observed no age reversal between any adjacent ^{14}C dating. Moreover, linear interpolation of all the age points estimates a carbonate low and a shipboard measured magnetic susceptibility high [*Bassinot et al.*, 2002] interval in the Holocene part of the core near 7.3 ka ago, which is very close to a volcanic eruption event, the “Kikai-Ah” in Japan [*Machida*, 2002] (Figure 4). The agreement of ages by a correction of 400 reservoir years differs from the 700 years used in one northern OT core study [*Sun et al.*, 2005], which may reflect different resolutions of the two cores. Although the reservoir age of the surface water of the western Pacific may vary in time

and space, our calibration schemes work well for the age model development of core MD012404, and suggest that the bottom of the core reaches back to the late MIS 5, or approximately 97 ka ago. Given the different construction methods of the age models, however, we consider that the uncertainty of age estimation for the core varies from a few hundred years (0–40 ka ago) to ~5 ka (40 ka ago, the core bottom).

3. Results

3.1. Foraminifer Isotopes

[11] The benthic oxygen isotope record of core MD012404 covers the late MIS 5 to MIS 1, the Holocene (Figure 3), on the basis of the results of planktic foraminifer AMS ^{14}C dating and benthic isotope stratigraphy [*Martinson et al.*, 1987]. The minima and maxima shown in the benthic isotope curve were picked up as MIS age control points (Figure 3). We have identified age control points MIS 3.13, 3.3, 3.31, 4.22, 4.24, 5.1, and 5.2 [*Martinson et al.*, 1987] in our benthic isotope curve, while attempting to maintain an overall match of these two curves (Figure 3). In the interval corresponding to MIS 3 (~40–60 ka ago), the benthic isotope curve of MD012404 appears to contain more millennial-scale isotope maxima and minima than those in the stack curve. The different resolutions of two curves increase the difficulty of the wiggle match and thus increase the uncertainty of the age model for this particular time interval. We consider that the uncertainty of the age model in such an interval (i.e., 40–60 ka ago) should be somewhat larger than the average uncertainty of the stack curve (~5 ka). By our age model, the benthic isotopes become heavier from MIS 5 toward MIS 2, with the lightest value (3.2‰) at ~80 ka ago and the heaviest value (4.5‰) at ~18 ka ago. Although the measured isotope values are scattered in nearby samples, the general trend after five points smoothing is similar to the global ice volume/sea level changes in the Pacific [*Lea et al.*, 2002; *Waelbroeck et al.*, 2002]. From the LGM (defined as 19–23 ka ago) to the late Holocene (0–4 ka ago) intervals of the core, the benthic isotope values have become lighter by ~1.2‰, which is similar to the global average value [*Fairbanks*, 1989; *Schrag et al.*, 1996, 2002] (Figure 3). Superimposed on the long-term variation, the benthic isotopes show well-resolved millennial to possibly centennial variations of ~0.1–0.2‰. The heavy benthic isotope value 4.5‰ near

Figure 4. Multiproxies measured from MD012404 for evaluating monsoon precipitation and productivity changes over the past 100,000 years in the OT: (a) sedimentation rate; (b) reconstructed relative sea level (RSL) curve from 0 to 23 ka ago [*Yokoyama et al.*, 2000; *Clark and Mix*, 2002; *Lambeck et al.*, 2002; *Yokoyama et al.*, 2007] and 23–97 ka ago [*Yokoyama et al.*, 2001a, 2001b; *Thompson and Goldstein*, 2005]; (c) carbonate contents; (d) $\delta^{13}\text{C}_{\text{org}}$ [*Kao et al.*, 2006b]; (e) TOC contents compared with (f) 60°N boreal summer insolation (in blue), 30° May (in orange) and September (in pink) insolation variations [*Berger*, 1978]; (g) opal contents; and (h) $\Delta\delta^{18}\text{O}_{\text{P-W}}$ (in blue and purple). The residuals of planktic foraminifer $\delta^{18}\text{O}$ after subtracting the global ice volume component of $\delta^{18}\text{O}$ variations (1‰ $\delta^{18}\text{O}$ corresponds to a 100 m sea level change, from the compiled sea level curve in Figure 5) and the differences between benthic and planktic foraminifer oxygen isotopes ($\Delta\delta^{18}\text{O}_{\text{B-P}}$) (in black) are used as a proxy for hydrographic gradients between the surface and deep water and fluxes of freshwater output into the OT. Sea level estimates for each sample were calculated from the age model for the core using a linear interpolation of the sea level curve. (i) Comparison of the TOC and opal content and $\Delta\delta^{18}\text{O}$ variations to a composite $\delta^{18}\text{O}$ record from stalagmites from East China [*Wang et al.*, 2001; *Yuan et al.*, 2004; *Wang et al.*, 2005]. The dashed lines are correlations of millennial-scale warm events.

Table 1. Age Control Points Used to Derive Age Model of Core MD012404^a

Depth (cm)	AMS ¹⁴ C Age	Error ^b	Calendar Age (years)	Species
14.5	1,040	±70	769	<i>G. sacculifer</i>
104.5	2,350	±30	2,193	<i>G. sacculifer</i> + <i>G. ruber</i>
254.5	4,500	±110	4,891	<i>G. sacculifer</i>
349.5	6,450	±30	7,202	<i>G. sacculifer</i> + <i>G. ruber</i>
494.5	9,730	±120	10,863	<i>G. sacculifer</i>
589.5	10,820	±190	12,585	<i>G. sacculifer</i>
624.5	11,370	±40	13,112	<i>G. sacculifer</i> + <i>G. ruber</i>
744.5	12,680	±130	14,620	<i>G. sacculifer</i>
854.5	13,950	±90	16,514	<i>G. sacculifer</i>
904.5	14,560	±45	17,407	<i>G. sacculifer</i> + <i>G. ruber</i>
1,019.5	15,810	±160	18,843	<i>G. sacculifer</i>
1,194.5	19,520	±230	23,057	<i>G. sacculifer</i>
1,379.5	21,360	±70	25,382	<i>G. sacculifer</i> + <i>G. ruber</i>
1,454.5	23,230	±270	27,561	<i>G. sacculifer</i>
1,539.5	24,450	±490	28,912	<i>G. sacculifer</i>
1,719.5	27,970	±200	32,554	<i>G. sacculifer</i> + <i>G. ruber</i>
1,914.5	30,200	±230	35,051	<i>G. sacculifer</i> + <i>G. ruber</i>
2,074.5	32,490	±1,110	37,252	<i>G. sacculifer</i> + <i>G. ruber</i>
2,174.5	34,010	±280	38,830	<i>G. sacculifer</i> + <i>G. ruber</i>
2,429.5			43,880	MIS 3.13
2,809.5			50,210	MIS 3.3
3,004.5			55,450	MIS 3.31
3,139.5			64,090	MIS 4.22
3,474.5			70,820	MIS 4.24
3,824.5			79,250	MIS 5.1
4,094.5			90,950	MIS 5.2

^aNineteen AMS ¹⁴C dated points were calibrated by using *Fairbanks et al.*'s [2005] function. The remaining seven points were graphic correlations based upon *Martinson et al.*'s [1987] data set that tuned by orbital forcing. MIS, marine isotope stage.

^bError is given in 1σ .

18 ka ago appears to be a millennial-scale event, but occurs ~2 ka before the abrupt cooling of Heinrich event 1 [*Bond et al.*, 1992]. This heavy value is similar to those reported from the southern OT cores [*Li et al.*, 1997, 2001], and may represent a millennial-scale deep water event. This heavy benthic isotope interval persists for >1 ka, which implies a large-scale oceanographic change that may have resulted from an intrusion of cold intermediate water from North Pacific high latitudes or a sinking of cold coastal water from the Yellow Sea during deglacial periods [*Ono et al.*, 2005]. In contrast to our planktic isotope curve, no deglacial reversal or Younger Dryas (YD) type of event was found in the benthic isotope record (Figure 3). This is consistent with what has been reported from a high-resolution benthic isotope study based on a marine core from the Pacific margin of Japan [*Oba et al.*, 2006]. In the Holocene, the benthic isotope record trends to heavier values from the late Holocene (~6 ka ago) toward the present, exhibiting also the same cooling trend shown in the northern high latitudes of the Holocene [*Fisher et al.*, 1998] (Figure 3).

[12] The planktic foraminifer isotope record measured from *G. ruber* of core MD012404 shows larger variations of ~0.4–0.5‰ of the high-frequency oscillations compared with the benthic record (Figure 3). Regional or local oceanographic effects that change the SST and/or SSS in the OT on these time scales must be taken into account for the variability. Moreover, from the LGM (defined as 19–23 ka ago) to the late Holocene (0–4 ka ago) intervals, the planktic isotope values have become lighter by ~1.7‰, which is similar to that have been observed in a nearby core from the OT [*Sun et al.*, 2005], and a core from the

northern ECS [*Ijiri et al.*, 2005]. The 1.7‰ change from the LGM to the late Holocene is larger than the global ice volume signal [*Fairbanks*, 1989; *Schrag et al.*, 1996, 2002]. This suggests that the planktic isotope changes, after subtracting the ice volume signal, may leave room for possible surface hydrographic (SSS and SST) changes.

[13] In this study, we use the differences between the planktic and benthic oxygen isotopes ($\Delta\delta^{18}\text{O}_{\text{B-P}}$) to estimate surface hydrographic changes in the seawater of the OT, by assuming that global ice volume drives similar changes in both records (Figure 4). Larger differences may be interpreted as larger gradients in T-S conditions between the bottom and surface water, reflecting warmer and/or fresher surface water conditions in the OT. The global ice volume component is removed from the planktic isotope record using sea level curves [*Yokoyama et al.*, 2000, 2001a, 2001b; *Clark et al.*, 2002; *Clark and Mix*, 2002; *Lambeck et al.*, 2002; *Thompson and Goldstein*, 2005; *Yokoyama et al.*, 2007] (Figure 4), which reflects the planktic isotope changes due only to local SST and/or SSS ($\Delta\delta^{18}\text{O}_{\text{P-W}}$). When calculating both of the $\Delta\delta^{18}\text{O}$, we observed clearly millennial-scale variability throughout the record (Figures 4 and 5). The millennial-scale variability shown in the $\Delta\delta^{18}\text{O}$ reaches or is greater than ~0.5‰, which could be translated into a minimum of ~2°C or ~1 psu [*Shackleton*, 1974; *Oba*, 1990; *Shimamura et al.*, 2005], or a combination of both changes in OT surface water. Standard methods that exist for estimating SSS in paleoceanography involve extracting ice volume and SST influences from planktic foraminifer $\delta^{18}\text{O}$, and explaining the residual of $\delta^{18}\text{O}$ in terms of SSS on the basis of the modern

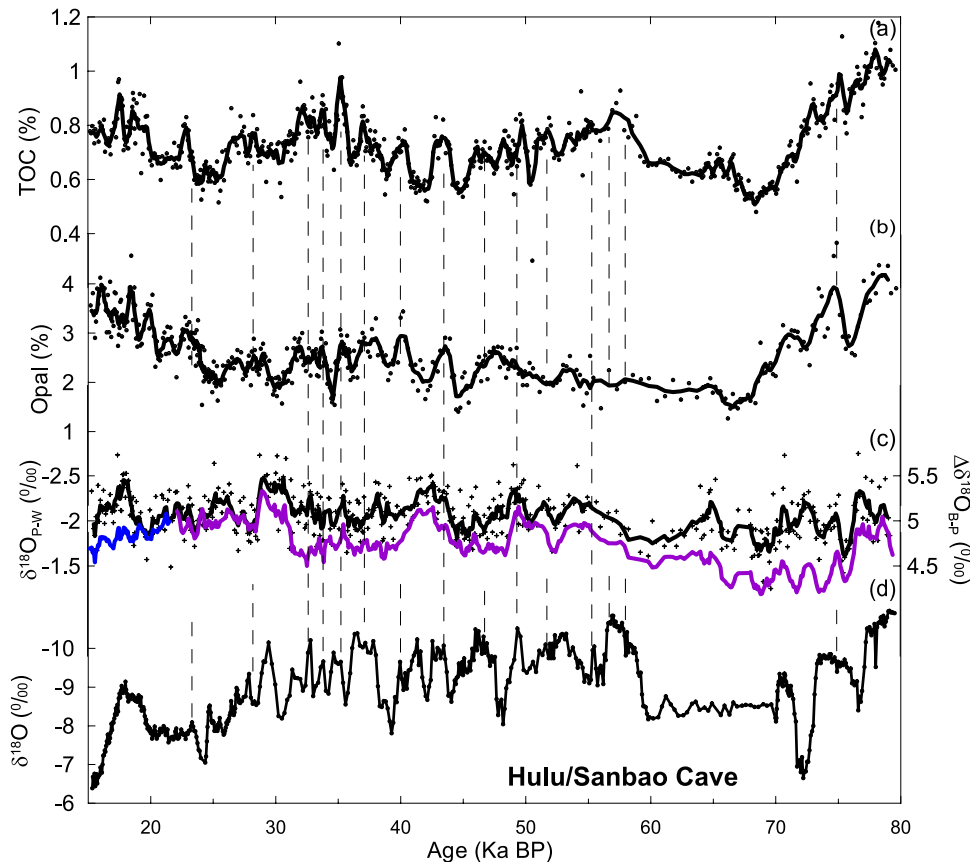


Figure 5. An enlarged version of a plot demonstrating the millennial-scale correlation of TOC and opal contents and $\Delta\delta^{18}\text{O}$ variations with a composite $\delta^{18}\text{O}$ record from stalagmites from East China [Wang *et al.*, 2001; Yuan *et al.*, 2004; Wang *et al.*, 2005]. The dashed lines are indicative of millennial-scale warm events.

relationship of $\delta^{18}\text{O}$ and SSS in seawater. While a full estimate of SST for this core is not available, our initial results using planktic foraminifer fauna assemblages indicate relatively high SSTs during interstadials but with small variability ($<1-1.5^\circ\text{C} \pm 1^\circ\text{C}$ in annual average, or $<1^\circ\text{C} \pm 1^\circ\text{C}$ in summer) [Chang *et al.*, 2008], which leaves room for interpreting the millennial-scale changes of $\Delta\delta^{18}\text{O}$ as contributed by SSS. The fauna SST variability shown here is slightly smaller than that reported when using *G. ruber* Mg/Ca from an OT core [Sun *et al.*, 2005]. Although proxy-dependent differences of SST exist between fauna and Mg/Ca methods [Steinke *et al.*, 2008], the millennial-scale variability shown in our $\Delta\delta^{18}\text{O}$ records may not be explained fully by SST changes in the ECS. Thus our millennial-scale $\Delta\delta^{18}\text{O}$ changes may reflect a combined effect from both SSS and SST changes, nevertheless indicating that major climate and oceanographic changes were felt in the surface water of the OT during this time interval.

3.2. Biogenic Components

[14] We have measured a combination of biogenic sediment and organic matter proxies from core MD012404 in an attempt to assess the impact of the monsoon and its changes on productivity in the surface water of the OT (Figure 4). Positive correlations between surface productivity and

buried organic matter have been documented previously [Froelich, 1980; Sheu *et al.*, 1995; Calvert, 1996; Agnihotri *et al.*, 2003; Jin *et al.*, 2006]. The use of this multiproxy approach helps us assess any common pattern associated with productivity changes among different biogenic proxies that are probably related to the combined effects of productivity, preservation (dissolution), diagenesis, and differential shelf export (lateral transport) from the Changjiang in the marginal sea.

[15] The carbonate contents display lower values in glacial stages and higher values in interglacial stages (Figure 4). MIS 5 is characterized by the highest carbonate content in the record, with a mean value of $\sim 26\%$. The carbonate contents have a mean value of $\sim 19\%$ in MIS 1, which is significantly higher than the glacial mean value of $\sim 14\%$. The carbonate content variation also mimics global sea level changes. This pattern suggests that the low-frequency component of carbonate content variations in the OT is mainly driven by terrestrial sediment dilution, not carbonate dissolution. Relatively high sedimentation rates during the glacial period also provide another indication of the terrestrial dilution effect during the glacial (Figure 4). Several sharp decreases in the carbonate contents are observed at 7.3, 29, 55, and 94 ka ago in the record, on the basis of our AMS ^{14}C and oxygen isotope age model.

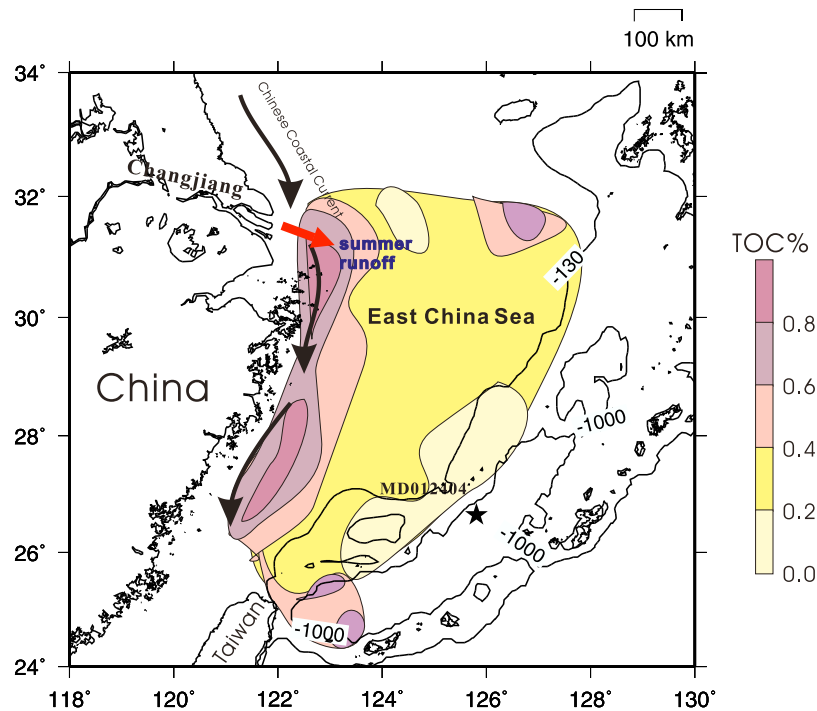


Figure 6. A map showing the TOC distribution in ECS surface sediments (data adopted from *Kao et al.* [2003]), suggesting that high TOC contents are confined to the Changjiang river mouth and on the shelf areas, indicating less terrestrial TOCs are transported from the Changjiang to the OT [*Kao et al.*, 2003].

Shipboard measured magnetic susceptibility data also show high values corresponding to the carbonate content lows [*Bassinot et al.*, 2002]. The timing of some of these carbonate content lows coincides with those of volcano eruptions that are dated as Kikai-Ah (7.3 ka ago), Aira-Tn (26~29 ka ago), and Kikai-Tz (95 ka ago) on the islands of Japan [*Machida*, 2002]. We speculate that there has been a long-range transport of the volcanic eruptive particles to the central OT, although direct evidence of the mineralogy or geochemistry of these tephra layers is not available and awaits future studies.

[16] The TOC contents reveal a range from 0.25 to 1.2%. They have been calculated as a carbonate-free basis for removing the dilution effect by carbonate contents. Higher TOC values are observed in MIS 5 and late MIS 2, but values are relatively low in the late Holocene and late MIS 4. High TOC contents are observed in broad intervals near ~80–90, 60, 36, and 10 ka ago on the basis of our ^{14}C and oxygen isotope age model. The variation of the TOC does not appear to be closely associated with changes in global ice volume, but follows those in summer insolation at 60°N [*Berger*, 1978], which exhibits ~21 ka precession cycles. Moreover, some TOC maxima or minima correspond more closely to late spring or early fall insolation variations at low latitude. For example, we observe that the TOC maxima at 32 ka ago are associated with May insolation maxima at 30°N ; and the TOC maxima and minima at 80–90 ka ago are linked to September insolation maxima and minima at 30°N (Figure 4). Superimposed on the orbital-scale variations, the TOC displays millennial-scale fluctuations (Figure 5). In the modern surface sediments of the OT and

ECS [*Kao et al.*, 2003] (Figure 6), high TOC contents restrict their distribution only near the Changjiang river mouth and on the shelf areas, indicating fewer terrestrial TOCs are transported from the Changjiang to the OT (Figure 6). Moreover, the carbon isotopes of organic matter ($\delta^{13}\text{C}_{\text{org}}$) measured from the bulk sediments of core MD012404 (Figure 4) [*Kao et al.*, 2006b] indicate a range of values from -20.6% to -21.8% , which also points to a dominant marine origin for the organic matter deposited at this site. Therefore we consider that the TOC content measured from core MD012404 is mainly an indicator of marine productivity, although a minor component of the TOC content is possibly of terrestrial origin or is exported from the Changjiang.

[17] Opal content is often used to refer to high productivity in surface oceans because siliceous microorganisms such as diatoms and radiolarians are major contributors of opal. Siliceous supply from local volcanic activities may change the saturation as well as the preservation level of opal in bottom water. The opal contents of MD012404 (Figure 4) have been recalculated on a carbonate-free basis. The opal contents range from 1.1 to 3.9%, with an average value of 2.1% in the record. Relatively high values for opal content are observed in MIS 5 and MIS 2, but low and stable values typify the Holocene and late MIS 4. Like that shown in the TOC record, high opal content is observed in the broad intervals of ~75–85, 50–55, 38–42, and 15–20 ka ago (Figure 4). The variation in the opal content appears to be tightly coupled with neither global ice volume nor insolation changes, but displays more clearly millennial-

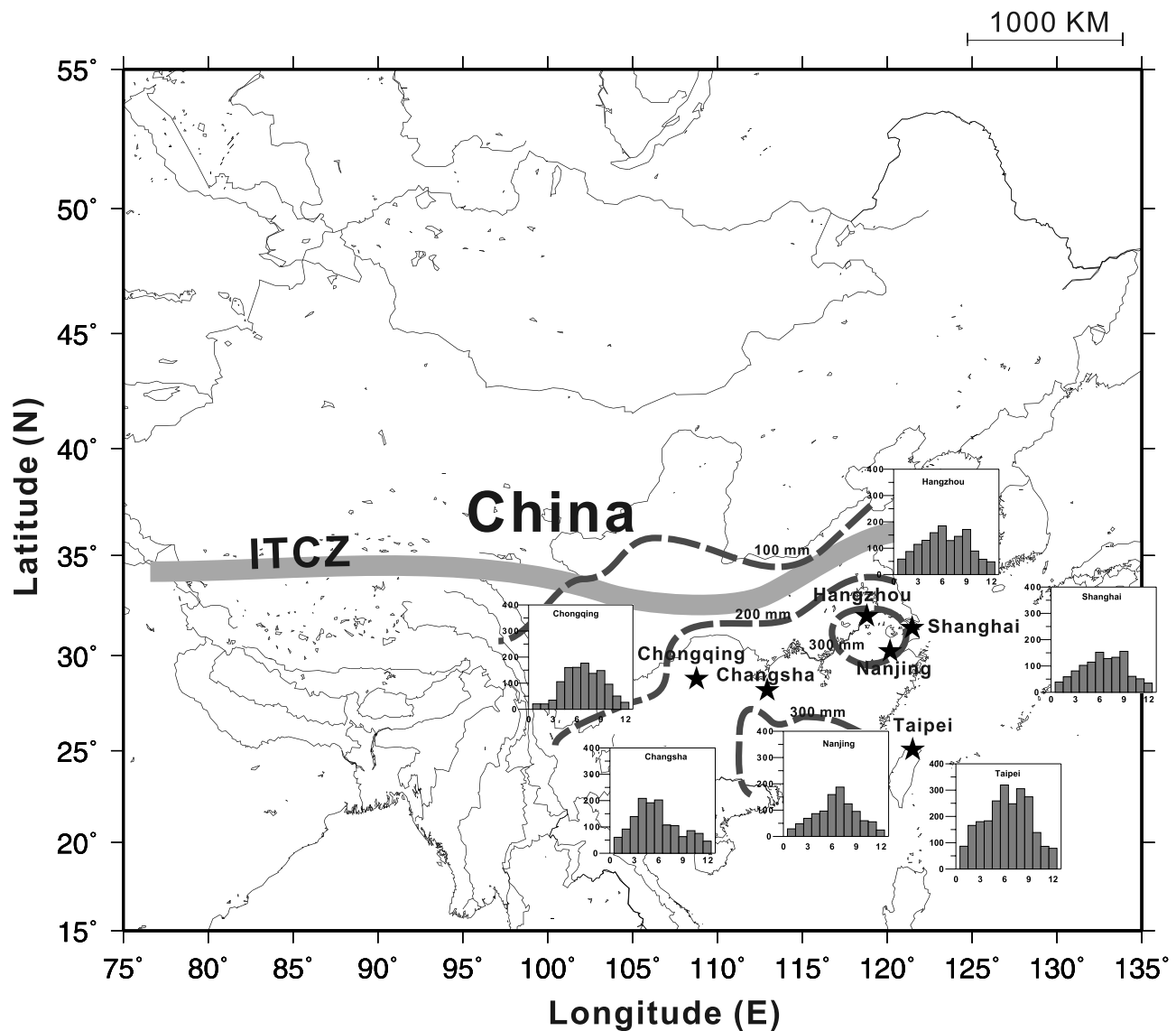


Figure 7. Monthly mean precipitation pattern (1971–2000) at six cities located adjacent to the heavy monsoon rain belt or in the catchment area of the Changjiang (data source, <http://cdc.cma.gov.cn/>). High precipitation reflects the latitudes of the Intertropical Convergence Zone (ITCZ) and the stationarity of Mei-Yu fronts.

scale fluctuations (Figure 5), irrespective of the glacial or interglacial stages.

4. Discussion

[18] Our multiproxy study on ECS core MD012404 reveals persistent orbital- to millennial-scale surface hydrography and productivity changes in the ECS over the past ~ 100 ka. Three major processes are possibly responsible for the observed patterns of change: (1) changes in precipitation and Changjiang freshwater inflow caused by monsoons and/or other climatic factors in East Asia; (2) marine productivity changes induced possibly by Kuroshio intermediate water (KIW) upwelling, which is in

response to the freshwater fluxes from land; and (3) sea level or possible tectonic setting changes in the OT.

[19] The intensity, duration, and spatial distribution of precipitation in the catchment area of the Changjiang determine the output of the freshwater runoff from the Changjiang into the ECS. Although interaction or feedback mechanisms involving evaporation, water vapor transport, wind field, topography and vegetation effects may all play a role in controlling the land precipitation, one 30-year (1971–2000) monthly and yearly precipitation record (<http://cdc.cma.gov.cn/>) indicates that the summer season, especially June, is the wettest period in the Changjiang basin, and the average precipitation is greater than 200 mm (Figure 7). From spring to summer, increased boreal solar insolation strengthens the monsoon winds, which bring heat

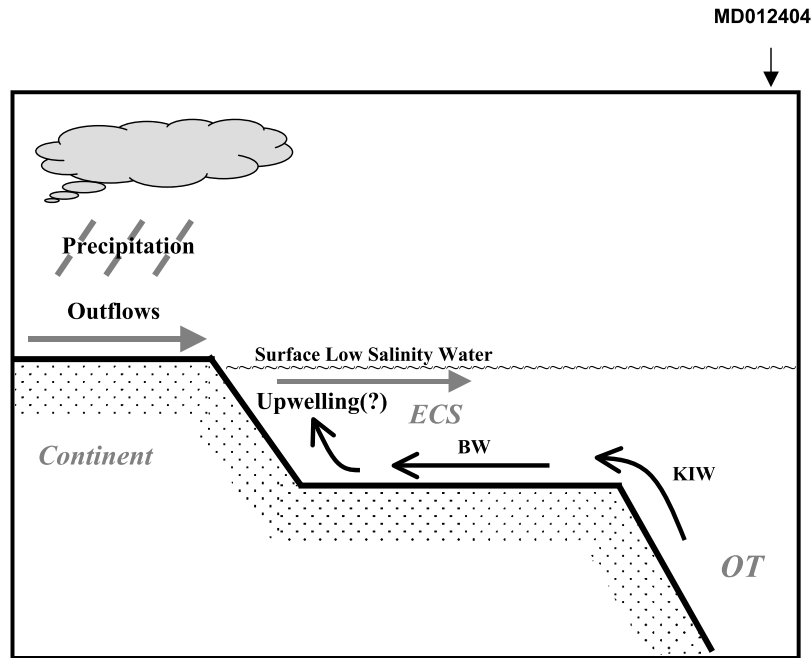


Figure 8. A simple conceptual model for the linkage between the freshwater inflow from the Changjiang and productivity in the East China Sea (ECS). Enhanced monsoon precipitation in the catchment area of the Changjiang increases the freshwater outflows into the ECS. The freshwater inflow from the Changjiang maintains the upwelling of Kuroshio intermediate water (KIW) that enters as bottom water (BW) on the shelf and in turn increases nutrient and productivity levels in the ECS.

and moisture into the interior of Asia. During these seasons, the Intertropical Convergence Zone (ITCZ) starts to shift to higher latitudes and reaches Changjiang catchment areas; meanwhile, the warm, humid maritime tropical air mass encounters the cold, dry continental air mass from Siberia, which in turn induces the formation of a stationary front that is accompanied by heavy precipitation (Mei-Yu) (Figure 7). The stationarity of the Mei-Yu rain belt is therefore another mechanism that brings heavy rainfall into the catchment basin of the Changjiang, and increases the freshwater discharge as well as sediment transport into the ECS. One long-term observation of rainfall patterns has also suggested that the El Niño–Southern Oscillation (ENSO) is closely linked to the precipitation in the catchment of the Changjiang [Zhang *et al.*, 2007]. All these climatological observations here suggest that changes in Changjiang catchment precipitation, which respond to the seasonal distribution of insolation in boreal summer and the onset of the East Asian monsoon [Liu *et al.*, 2007], must be one of the most important factors controlling the SSS in the ECS.

[20] Marine productivity plays an important role in contributing organic matter that sinks into the ECS. A sufficient supply of dissolved inorganic nutrients is a key factor controlling the productivity of the ocean. Mean primary productivity in the ECS is $425 \text{ mg m}^{-2} \text{ d}^{-1}$ (varies from 108 to $997 \text{ mg m}^{-2} \text{ d}^{-1}$), and thus the ECS is one of the most productive areas in the world, serving as a sink in global biogeochemical cycles [Gong *et al.*, 2003]. Satellite data have shown that sea surface productivity in the ECS is higher in the summer and the productive maximum is

observed in the coastal area around the estuary of the Changjiang, accompanied by a SST high and SSS low [Gong *et al.*, 2003]. The discharge of nutrients from the Changjiang has long been considered a main source of nutrient input to the ECS [Beardsley *et al.*, 1985]. Previous studies have suggested that the suspended matter in the ECS was blocked by upwelling water from the Kuroshio during the summer, which could be transported to the OT only during the winter because of the retreat of upwelled water back to the OT and more intense surface water mixing caused by cold winds [Milliman *et al.*, 1985b, 1985a]. However, more recent studies using box model calculations [Chen, 1996; Chen *et al.*, 2004] have suggested that the KIW (Kuroshio intermediate water), which was upwelled to the continental shelf during the summer season, might serve as the dominant route of nutrient supply in the ECS (Figure 8). A salt balance process between bottom water from the KIW and low-salinity surface water that inflows from the Changjiang estuary might function as a driving force to increase the nutrient upwelling on the continental shelf [Chen and Wang, 1999; Chen, 2000]. In this model, an increased freshwater inflow from the Changjiang brings up more nutrients from deeper water, and consequently the high nutrient level intensifies the surface productivity in the ECS. A 10% decrease of freshwater outflow from the Changjiang will reduce approximately 9% of the cross-shelf water exchange and onshore nutrient supply as well [Chen, 2000]. These oceanographic observation and modeling studies support the view that Changjiang freshwater outflow and possibly its induced KIW upwelling [Chen, 1996; Chen

et al., 2004] play a role in controlling the timing of ECS productivity variations on orbital to millennial scales. These studies leave room for further investigation of the geochemical evidence that links to the past dynamics of KIW upwelling.

[21] Besides the monsoon precipitation, the changes in sea level also may have influenced the productivity or preservation of biogenic sediments and organic matter in the OT, since a sea level drop may block the intrusion of the Kuroshio into the OT through a gateway near Ryukyu Island or the Yonaguni Depression area around northeastern Taiwan (Figure 1). Reduced intrusion of the Kuroshio water may reduce the ventilation of deep water in the OT, thus favoring the preservation of biogenic sediments and organic matter. One model study [Kao *et al.*, 2006b] has suggested that the Kuroshio intrusion was not significantly reduced until the sea level was set at 135 m below the present level. Such low sea level conditions only happen in MIS 2 during the time scale of our study. Several hypotheses call upon tectonic barriers near the southern Ryukyu or at the Yonaguni Depression [Ujiié *et al.*, 1991; Kao *et al.*, 2006a] that may have efficiently blocked the intrusion of the Kuroshio before ~80 ka ago, but this awaits further investigation for evidence.

[22] Our study documents that the orbital-scale productivity changes (in TOC content) in the ECS is more tightly linked to boreal summer (from May to September) insolation variations that exhibit precession cycles of ~21 ka [Berger, 1978] (Figure 4). The timing of the maximum productivity in the ECS at ~10 and 55 ka ago observed here coincides with the timing of maximum average insolation of summer (June, July, and August) (Figure 4). This observation is consistent with what has been suggested in SCS or Sulu Sea studies that summer monsoon maxima occurred in peak climate warming [Oppo *et al.*, 2003; Yu *et al.*, 2006]. However, our observation also indicates that the ECS productivity variations of some time intervals appear to be linked more closely to late spring or early fall insolation at low latitudes. For example, a productivity maximum at ~35 ka ago appears to be linked more tightly to a May insolation maximum, and productivity minimum at ~85 ka ago seems to coincide with a September insolation minimum (Figure 4). The varied timing of orbital-scale responses of the monsoon productivity variations observed here suggests that the monsoon precipitation is probably controlled by more complicated mechanisms in East Asia. In particular, the coincidence between the maxima and minima in our monsoon productivity indicators with respect to May and September insolation changes implies that other mechanisms for intensifying precipitation in East Asia such as the late spring Mei-Yu rain belt associated with stationary fronts, and/or more heavy rainy storms brought by typhoons (tropical hurricane) in late summer in the western Pacific, are probably effective as well. We speculate that insolation maxima of precession cycles in May or September may trigger more intensified and/or prolonged Mei-Yu or typhoon seasons, which could raise precipitation level on land, that in turn, elevate the productivity in the surface ocean to as high as that during the summer monsoon seasons from June to August. If this is an explanation for

the varied timing of orbital response of productivity that observed in this study, our data thus suggest a strikingly thermal response of precipitation to May or September insolation maxima on precession cycle in East Asia. In contrast to the large responses of precession cycles shown in our productivity record, the variations of precession cycles in our $\Delta\delta^{18}\text{O}$ is minimal. The instance indicates that the $\Delta\delta^{18}\text{O}$ changes may not solely reflect monsoon-induced salinity changes in our study area. Other processes, such as varied shifting of precipitation from land to sea depending on the strength of summer monsoons [Oppo *et al.*, 2003; Oppo and Sun, 2005] and of source or transport path of precipitation water $\delta^{18}\text{O}$ in East Asia, and the local SST change and/or advection in subsurface waters, maybe involved in modifying the $\Delta\delta^{18}\text{O}$.

[23] Our records demonstrate a striking correlation with global millennial-scale climatic events in the western Pacific paleoclimate, as shown previously in Japan Sea studies [Tada *et al.*, 1999; Tada, 2004]. The timing of low SSS (and possibly high SST as well) and productivity coincides with the strong monsoon episodes on millennial scales in the stalagmite records [Wang *et al.*, 2001; Yuan *et al.*, 2004; Wang *et al.*, 2005] (Figures 4 and 5). Since the MD012404 and stalagmite records are dated independently, the correlation is not likely to have resulted from any artifacts in our methods. Our comparison suggests that on a millennial scale, strong monsoon events recorded by the $\delta^{18}\text{O}$ minima of stalagmite records correlate tightly with the maxima of TOC and opal contents, though the correlations to $\delta^{18}\text{O}_{\text{P-W}}$ and $\delta^{18}\text{O}_{\text{B-P}}$ are not as high as those to the TOC and opal contents, indicating probably the foraminiferal oxygen isotopes are not straightforward monsoon-induced salinity indicators as we explained in our previous discussion on precession cycles. This study, however, suggests that the climate changes over millennial scales are expressed strongly in land and sea in East Asia. The abrupt changes of $\delta^{18}\text{O}_{\text{P-W}}$ and $\delta^{18}\text{O}_{\text{B-P}}$ shown in our record also appear to be dominant and persistent features, irrespective of local sea level changes. Our observation here highlights the importance of proposed mechanisms of millennial-scale changes that link the surface water hydrology in the tropics and the thermohaline circulation in the North Atlantic [Schmittner and Clement, 2002; Zhang and Delworth, 2005]. However, we caution that our age model for the interval between 40 and 60 ka ago is subject to a larger interpretation error (>5 ka), which makes our correlation for this interval more uncertain.

5. Conclusions

[24] Our OT core studies suggest that the surface hydrography and productivity changes (estimated by using various proxies based on foraminifer isotopes, biogenic sediment components, and organic matter from the core) exhibit noticeable orbital and millennial-scale variations in the ECS of the past 100,000 years. These are related to the combined effects of (1) changes in precipitation and Changjiang freshwater inflow caused by monsoons and/or other climatic factors in East Asia and (2) marine productivity changes induced possibly by KIW upwelling, which is in response to

the freshwater fluxes from land. The most remarkable feature of the variability shown in the records is the nearly synchronous, millennial-scale changes in the ECS surface hydrography and productivity coincident with monsoon events in the Hulu/Dongge stalagmite isotope records. Increased freshening and high productivity correlate with high monsoon intensity in interstadials. This suggests that the changes of surface hydrography and productivity in the ECS are driven mainly by monsoon processes, and are probably persistent features that are independent of glacial or interglacial stages. On orbital time scales, our reconstructed productivity (TOC) changes coincide with the increases of boreal May–September insolation driven by precession cycles (~21 ka). One possible mechanism for pacing the synchronous changes between boreal insolation and ECS surface productivity is related to KIW upwelling changes that occur in response to freshwater inflow variations from the Changjiang. This implies that land precipitation might be responsible for the observed high productivity. Our productivity and $\delta^{18}\text{O}$ records, however, suggest that the precipitation and SSS patterns in the ECS may have been controlled by more complicated mechanisms. Although we recognize that there is a larger dating

uncertainty in the interval of 40–60 ka ago, we have demonstrated a high-resolution correlation between the land and the marine monsoon records and underscore the need for more records or proxies that could be used to probe the dynamics of ocean processes that respond to monsoon variability.

[25] **Acknowledgments.** This study was supported by National Taiwan Ocean University and a grant (NSC95-2611-M-019-013) from the National Science Council, Taiwan. The authors would like to thank Delia Oppo and Ryuji Tada for many stimulating discussions and thorough reviews on an early version of the manuscript. Sincere thanks go to the crew of the R/V *Marion Dufresne* for their coring assistance. Members who work in the Core Repository and Laboratory at the National Center for Ocean Research are also due our thanks for helping us finish the measurements in this study. Special thanks go to the staff of the Earth and Planetary System Science Group in the Department of Earth and Planetary Science and Micro Analysis Laboratory, Tandem Accelerator, at the University of Tokyo, who helped us finish the experiments that required AMS ^{14}C dating. All stable isotope measurements were completed at the Geological Survey of Japan at the National Institute of Advanced Industrial Science and Technology, Japan, and all the members there are thanked here for their generous assistance. Y.Y.'s work was partly supported by Global Environmental Research Fund (RF-081) and JSPS Kakenhi (21674003).

References

- Agnihotri, R., M. M. Sarin, B. L. K. Somayajulu, A. J. T. Jull, and G. S. Burr (2003), Late-Quaternary biogenic productivity and organic carbon deposition in the eastern Arabian Sea, *Palaeogeogr. Palaeoclimatol. Palaeoecol.*, **197**, 43–60, doi:10.1016/S0031-0182(03)00385-7.
- Bassinot, F. C., et al. (2002), Scientific report of the WEPAMA cruise, MD122/IMAGES VII, 453 pp., Inst. Fr. Pour la Rech. et la Technol. Polaires, Plouzané, France.
- Beardsley, R. C., R. Limeburner, H. Yu, and G. A. Cannon (1985), Discharge of the Changjiang (Yangtze River) into the East China Sea, *Cont. Shelf Res.*, **4**, 57–76, doi:10.1016/0278-4343(85)90022-6.
- Berger, A. L. (1978), Long-term variations of caloric insolation resulting from the Earth's orbital elements, *Quat. Res.*, **9**, 139–167, doi:10.1016/0033-5894(78)90064-9.
- Bond, G., et al. (1992), Evidence for massive discharges of icebergs into the North Atlantic Ocean during the last glacial period, *Nature*, **360**, 245–249, doi:10.1038/360245a0.
- Bush, A. B. G., and R. G. Fairbanks (2003), Exposing the Sunda shelf: Tropical responses to eustatic sea level change, *J. Geophys. Res.*, **108**(D15), 4446, doi:10.1029/2002JD003027.
- Bush, A. B. G., and S. G. H. Philander (1999), The climate of the Last Glacial Maximum: Results from a coupled atmosphere-ocean general circulation model, *J. Geophys. Res.*, **104**(D20), 24,509–24,525, doi:10.1029/1999JD900447.
- Calvert, S. E. (1996), Influence of water column anoxia and sediment supply on the burial and preservation of organic carbon in marine shales, *Geochim. Cosmochim. Acta*, **60**(9), 1577–1593, doi:10.1016/0016-7037(96)00041-5.
- Chang, Y.-P., S.-M. Wu, K.-Y. Wei, M. Murayama, H. Kawahata, and M.-T. Chen (2005), Foraminiferal oxygen isotope stratigraphy and high-resolution organic carbon, carbonate records from the Okinawa Trough (IMAGES MD012404 and ODP Site 1202), *Terr. Atmos. Oceanic Sci.*, **16**(1), 57–73.
- Chang, Y.-P., W.-L. Wang, Y. Yokoyama, H. Matsuzaki, H. Kawahata, and M.-T. Chen (2008), Millennial-scale planktic foraminifer sea surface temperature variability in the East China Sea of the past 40,000 years (IMAGES MD012404 from the Okinawa Trough), *Terr. Atmos. Oceanic Sci.*, **19**(4), 389–401, doi:10.3319/TAO.2008.19.4.389(IMAGES).
- Chen, C.-T. A. (1996), The Kuroshio intermediate water is the major source of nutrients on the East China Sea continental shelf, *Oceanol. Acta*, **19**, 523–527.
- Chen, C.-T. A. (2000), The Three Gorges Dam: Reducing the upwelling and thus productivity in the East China Sea, *Geophys. Res. Lett.*, **27**(3), 381–383, doi:10.1029/1999GL002373.
- Chen, C.-T. A., and S.-L. Wang (1999), Carbon, alkalinity and nutrient budgets on the East China Sea continental shelf, *J. Geophys. Res.*, **104**(C9), 20,675–20,686, doi:10.1029/1999JC900055.
- Chen, M.-T., and C.-Y. Huang (1998), Ice-volume forcing of winter monsoon climate in the South China Sea, *Paleoceanography*, **13**(6), 622–633, doi:10.1029/98PA02356.
- Chen, Y.-L. L., H.-Y. Chen, G.-C. Gong, Y.-H. Lin, S. Jan, and M. Takahashi (2004), Phytoplankton production during a summer coastal upwelling in the East China Sea, *Cont. Shelf Res.*, **24**, 1321–1338, doi:10.1016/j.csr.2004.04.002.
- Cheng, H., R. L. Edwards, Y. Wang, X. Kong, Y. Ming, M. J. Kelly, X. Wang, C. D. Gallup, and W. Liu (2006), A penultimate glacial monsoon record from Hulu Cave and two-phase glacial terminations, *Geology*, **34**(3), 217–220, doi:10.1130/G22289.1.
- Clark, P. U., and A. C. Mix (2002), Ice sheets and sea level of the Last Glacial Maximum, *Quat. Sci. Rev.*, **21**, 1–7, doi:10.1016/S0277-3791(01)00118-4.
- Clark, P. U., J. X. Mitrovica, G. A. Milne, and M. E. Tamisiea (2002), Sea-level fingerprinting as a direct test for the source of global meltwater pulse 1A, *Science*, **295**, 2438–2441.
- Clemens, S., W. Prell, D. Murray, G. Shimmiel, and G. Weedon (1991), Forcing mechanisms of the Indian Ocean monsoon, *Nature*, **353**, 720–725, doi:10.1038/353720a0.
- Clemens, S., P. Wang, and W. Prell (2003), Monsoons and global linkages on Milankovitch and sub-Milankovitch time scales, *Mar. Geol.*, **201**(1–3), 1–3, doi:10.1016/S0025-3227(03)00195-6.
- Dannenmann, S., B. K. Linsley, D. W. Oppo, Y. Rosenthal, and L. Beaufort (2003), East Asian monsoon forcing of suborbital variability in the Sulu Sea during marine isotope stage 3: Link to Northern Hemisphere climate, *Geochim. Geophys. Geosyst.*, **4**(1), 1001, doi:10.1029/2002GC000390.
- Fairbanks, R. G. (1989), A 17,000-year glacio-eustatic sea level record: Influence of glacial melting rates on the Younger Dryas event and deep-ocean circulation, *Nature*, **342**, 637–642, doi:10.1038/342637a0.
- Fairbanks, R. G., R. A. Mortlock, T.-C. Chiu, L. Cao, A. Kaplan, T. P. Guilderson, T. W. Fairbanks, A. L. Bloom, P. M. Grootes, and M.-J. Nadeau (2005), Radiocarbon calibration curve spanning 0 to 50,000 years BP based on paired $^{230}\text{Th}/^{234}\text{U}$ and ^{14}C dates on pristine corals, *Quat. Sci. Rev.*, **24**, 1781–1796, doi:10.1016/j.quascirev.2005.04.007.
- Fisher, D. A., et al. (1998), Penny ice cap cores, Baffin Island, Canada, and the Wisconsinan Foxe Dome connection: Two states of Hudson Bay ice cover, *Science*, **279**, 692–695, doi:10.1126/science.279.5351.692.
- Froelich, P. N. (1980), Analysis of organic carbon in marine sediments, *Limnol. Oceanogr.*, **25**(3), 564–572.
- Gong, G.-C., Y.-H. Wen, B.-W. Wang, and G.-J. Liu (2003), Seasonal variation of chlorophyll *a* concentration, primary production and environmental conditions in the subtropical East China Sea, *Deep Sea Res., Part II*, **50**, 1219–1236, doi:10.1016/S0967-0645(03)00019-5.

- Hsu, S.-C., F.-J. Lin, W.-L. Jeng, and T. Y. Tang (1998), The effect of a cyclonic eddy on the distribution of lithogenic particles in the southern East China Sea, *J. Mar. Res.*, *56*, 813–832, doi:10.1357/002224098321667387.
- Ijiri, A., L. Wang, T. Oba, H. Kawahata, C.-Y. Huang, and C.-Y. Huang (2005), Paleo-environmental changes in the northern area of the East China Sea during the past 42,000 years, *Palaeogeogr. Palaeoclimatol. Palaeoecol.*, *219*, 239–261, doi:10.1016/j.palaeo.2004.12.028.
- Imbrie, J., J. D. Hays, D. G. Matinson, A. McIntyre, A. C. Mix, J. J. Morley, N. G. Pisias, W. L. Prell, and N. J. Shackleton (1984), The orbital theory of Pleistocene climate: Support from a revised chronology of the marine $\delta^{18}\text{O}$ record, in *Milankovitch and Climate*, edited by A. Berger et al., pp. 269–305, D. Reidel, Dordrecht, Netherlands.
- Jian, Z., P. Wang, Y. Saito, J. Wang, U. Pflaumann, T. Oba, and X. Cheng (2000), Holocene variability of the Kuroshio Current in the Okinawa Trough, northwestern Pacific Ocean, *Earth Planet. Sci. Lett.*, *184*(1), 305–319, doi:10.1016/S0012-821X(00)00321-6.
- Jin, X., N. Gruber, J. P. Dunne, J. L. Sarmiento, and R. A. Armstrong (2006), Diagnosing the contribution of phytoplankton functional groups to the production and export of particulate organic carbon, CaCO_3 , and opal from global nutrient and alkalinity distributions, *Global Biogeochem. Cycles*, *20*, GB2015, doi:10.1029/2005GB002532.
- Kao, S. J., F. J. Lin, and K. K. Liu (2003), Organic carbon and nitrogen contents and their isotopic compositions in surficial sediments from the East China Sea shelf and the southern Okinawa Trough, *Deep Sea Res., Part II*, *50*, 1203–1217, doi:10.1016/S0967-0645(03)00018-3.
- Kao, S. J., A. P. Roberts, S. C. Hsu, Y. P. Chang, W. B. Lyons, and M. T. Chen (2006a), Monsoon forcing, hydrodynamics of the Kuroshio Current, and tectonic effects on sedimentary carbon and sulfur cycling in the Okinawa Trough since 90 ka, *Geophys. Res. Lett.*, *33*, L05610, doi:10.1029/2005GL025154.
- Kao, S. J., C.-R. Wu, Y.-C. Hsin, and M. Dai (2006b), Effects of sea level change on the upstream Kuroshio Current through the Okinawa Trough, *Geophys. Res. Lett.*, *33*, L16604, doi:10.1029/2006GL026822.
- Kutzbach, J. E., and P. J. Guetter (1986), The influence of changing orbital parameters and surface boundary conditions on climate simulations for the past 18,000 years, *J. Atmos. Sci.*, *43*, 1726–1759, doi:10.1175/1520-0469(1986)043<1726:TIOCOP>2.0.CO;2.
- Lambeck, K., Y. Yokoyama, and T. Purcell (2002), Into and out of the Last Glacial Maximum: Sea-level change during oxygen isotope stages 3 and 2, *Quat. Sci. Rev.*, *21*, 343–360, doi:10.1016/S0277-3791(01)00071-3.
- Lea, D. W., P. A. Martin, D. K. Pak, and H. J. Spero (2002), Reconstructing a 350 ky history of sea level using planktonic Mg/Ca and oxygen isotope records from a Cocos Ridge core, *Quat. Sci. Rev.*, *21*, 283–293, doi:10.1016/S0277-3791(01)00081-6.
- Levitus, S., and T. P. Boyer (1994), *World Ocean Atlas 1994*, vol. 4, *Temperature*, NOAA Atlas NESDIS, vol. 4, 129 pp., NOAA, Silver Spring, Md.
- Li, B., Z. Jian, and P. Wang (1997), *Pulleniatina obliquoluculata* as a paleoceanographic indicator in the southern Okinawa Trough during the last 20,000 years, *Mar. Micropaleontol.*, *32*, 59–69, doi:10.1016/S0377-8398(97)00013-3.
- Li, T., Z. Liu, M. A. Hall, S. Berne, Y. Saito, S. Cang, and Z. Cheng (2001), Heinrich event imprints in the Okinawa Trough: Evidence from oxygen isotope and planktonic foraminifera, *Palaeogeogr. Palaeoclimatol. Palaeoecol.*, *176*, 133–146, doi:10.1016/S0031-0182(01)00332-7.
- Liang, W.-D., T. Y. Tang, Y. J. Yang, M. T. Ko, and W.-S. Chuang (2003), Upper-ocean currents around Taiwan, *Deep Sea Res., Part II*, *50*, 1085–1105, doi:10.1016/S0967-0645(03)00011-0.
- Liu, J., R. Zhu, T. Li, A. Li, and J. Li (2007), Sediment-magnetic signature of the mid-Holocene paleoenvironmental change in the central Okinawa Trough, *Mar. Geol.*, *239*(1–2), 19–31, doi:10.1016/j.margeo.2006.12.011.
- Machida, H. (2002), Volcanoes and tephra in the Japan area, *Global Environ. Res.*, *6*, 19–28.
- Martinson, D. G., N. G. Pisias, J. D. Hays, J. Imbrie, T. C. Moore Jr., and N. J. Shackleton (1987), Age dating and the orbital theory of the ice ages: Development of a high-resolution 0 to 300,000-year chronostratigraphy, *Quat. Res.*, *27*, 1–29, doi:10.1016/0033-5894(87)90046-9.
- Milliman, J. D., and R. H. Meade (1983), Worldwide delivery of river sediment to the oceans, *J. Geol.*, *91*, 1–21.
- Milliman, J. D., H. T. Shen, Z. S. Yang, and R. H. Meade (1985a), Transport and deposition of river sediment in the Changjiang estuary and adjacent continental shelf, *Cont. Shelf Res.*, *4*, 37–45, doi:10.1016/0278-4343(85)90020-2.
- Milliman, J. D., R. C. Beardsley, Z. Yang, and R. Limeburner (1985b), Modern Huanghe-derived muds on the outer shelf of the East China Sea: Identification and potential transport mechanisms, *Cont. Shelf Res.*, *4*, 175–188, doi:10.1016/0278-4343(85)90028-7.
- Mortlock, R. A., and P. N. Froelich (1989), A simple method for the rapid determination of biogenic opal in pelagic marine sediments, *Deep Sea Res., Part A*, *36*, 1415–1426, doi:10.1016/0198-0149(89)90092-7.
- Oba, T. (1990), Paleoceanographic information obtained by the isotopic measurement of individual foraminiferal specimens, paper presented at First International Conference on Asian Marine Geology, Tongji Univ., Shanghai, China, 7–10 Sept.
- Oba, T., T. Irino, M. Yamamoto, M. Murayama, A. Takamura, and K. Aoki (2006), Paleoceanographic change off central Japan since the last 144,000 years based on high-resolution oxygen and carbon isotope records, *Global Planet. Change*, *53*(1–2), 5–20, doi:10.1016/j.gloplacha.2006.05.002.
- Ono, A., K. Takahashi, K. Katsuki, Y. Okazaki, and T. Sakamoto (2005), The Dansgaard-Oeschger cycles discovered in the up stream source region of the North Pacific intermediate water formation, *Geophys. Res. Lett.*, *32*, L11607, doi:10.1029/2004GL022260.
- Oppo, D. W., and Y. Sun (2005), Amplitude and timing of sea-surface temperature change in the northern South China Sea: Dynamic link to the East Asian monsoon, *Geology*, *33*(10), 785–788, doi:10.1130/G21867.1.
- Oppo, D. W., B. K. Linsley, Y. Rosenthal, S. Dannenmann, and L. Beaufort (2003), Orbital and suborbital climate variability in the Sulu Sea, western tropical Pacific, *Geochem. Geophys. Geosyst.*, *4*(1), 1003, doi:10.1029/2001GC000260.
- Partin, J. W., K. M. Cobb, J. F. Adkins, B. Clark, and D. P. Fernandez (2007), Millennial-scale trends in West Pacific warm pool hydrology since the Last Glacial Maximum, *Nature*, *449*, 452–455, doi:10.1038/nature06164.
- Pisias, N. G., D. G. Matinson, T. C. Moore Jr., N. J. Shackleton, W. Prell, J. Hays, and G. Boden (1984), High resolution stratigraphic correlation of benthic oxygen isotopic records spanning the last 300,000 years, *Mar. Geol.*, *56*(1–4), 119–136, doi:10.1016/0025-3227(84)90009-4.
- Prell, W. L., and J. E. Kutzbach (1987), Monsoon variability over the past 150,000 years, *J. Geophys. Res.*, *92*(D7), 8411–8425, doi:10.1029/JD092iD07p08411.
- Schmittner, A., and A. C. Clement (2002), Sensitivity of the thermohaline circulation to tropical and high latitude freshwater forcing during the last glacial-interglacial cycle, *Paleoceanography*, *17*(2), 1017, doi:10.1029/2000PA000591.
- Schrag, D. P., G. Hampt, and D. W. Murray (1996), Pore fluid constraints on the temperature and oxygen isotopic composition of the glacial ocean, *Science*, *272*, 1930–1932, doi:10.1126/science.272.5270.1930.
- Schrag, D. P., J. F. Adkins, K. McIntyre, J. L. Alexander, D. A. Hodell, C. D. Charles, and J. F. McManus (2002), The oxygen isotopic composition of seawater during the Last Glacial Maximum, *Quat. Sci. Rev.*, *21*, 331–342, doi:10.1016/S0277-3791(01)00110-X.
- Shackleton, N. J. (1974), Attainment of isotopic equilibrium between ocean water and benthonic foraminifera genus *Uvigerina*: Isotopic changes in the ocean during the last glacial, in *Les Méthodes Quantitatives d'Étude des Variations du Climat au Cours du Pléistocène*, edited by J. Labeyrie, pp. 203–209, Colloq. Int. Cent. Natl. de la Rech. Sci., Paris.
- Sheu, D. D., W.-C. Jou, M.-J. Chen, W.-Y. Lee, and S. Lin (1995), Variations of calcium carbonate, organic carbon and their isotopic compositions in surface sediments of the East China Sea, *Terr. Atmos. Oceanic Sci.*, *16*(1), 115–128.
- Shimamura, M., T. Oba, G. Xu, B. Lu, L. Wang, M. Murayama, K. Toyoda, and A. Winter (2005), Fidelity of $\delta^{18}\text{O}$ as a proxy for sea surface temperature: Influence of variable coral growth rates on the coral *Porites lutea* from Hainan Island, China, *Geochem. Geophys. Geosyst.*, *6*, Q09017, doi:10.1029/2005GC000966.
- Sibuet, J.-C., B. Deffontaines, S. Hsu, N. Thureau, J. Le Formal, C. Liu, and A. Party (1998), Okinawa Trough backarc basin: Early tectonic and magmatic evolution, *J. Geophys. Res.*, *103*(B12), 30,245–30,267, doi:10.1029/98JB01823.
- Steinke, S., M. Kienast, J. Groeneveld, L.-C. Lin, M.-T. Chen, and R. Rendle-Bühning (2008), Proxy dependence of the temporal pattern of deglacial warming in the tropical South China Sea: Toward resolving seasonality, *Quat. Sci. Rev.*, *27*, 688–700, doi:10.1016/j.quascirev.2007.12.003.
- Sun, Y., D. W. Oppo, R. Xiang, W. Liu, and S. Gao (2005), Last deglaciation in the Okinawa Trough: Subtropical northwest Pacific link to Northern Hemisphere and tropical climate, *Paleoceanography*, *20*, PA4005, doi:10.1029/2004PA001061.
- Tada, R. (2004), Onset and evolution of millennial-scale variability in the Asian monsoon and its impact on paleoceanography of the Japan Sea, in *Continent-Ocean Interactions Within East Asian Marginal Seas*, *Geophys. Monogr. Ser.*,

- vol. 149, edited by P. Clift et al., pp. 283–298, AGU, Washington, D. C.
- Tada, R., T. Irino, and I. Koizumi (1999), Land-ocean linkages over orbital and millennial timescales recorded in late Quaternary sediments of the Japan Sea, *Paleoceanography*, *14*(2), 236–247, doi:10.1029/1998PA900016.
- Tang, T. Y., J. H. Tai, and Y. J. Yang (2000), The flow pattern north of Taiwan and the migration of the Kuroshio, *Cont. Shelf Res.*, *20*, 349–371, doi:10.1016/S0278-4343(99)00076-X.
- Thompson, W. G., and S. L. Goldstein (2005), Open-system coral ages reveal persistent sub-orbital sea-level cycles, *Science*, *308*, 401–404, doi:10.1126/science.1104035.
- Ujiié, H., Y. Tanaka, and T. Ono (1991), Late Quaternary paleoceanographic record from the middle Ryukyu Trench slope, north-west Pacific, *Mar. Micropaleontol.*, *18*, 115–128, doi:10.1016/0377-8398(91)90008-T.
- Waelbroeck, C., L. D. Labeyrie, E. Michel, J.-C. Duplessy, J. McManus, K. Lambeck, E. Balbon, and M. Labracherie (2002), Sea-level and deep water temperature changes derived from benthic foraminifera isotopic records, *Quat. Sci. Rev.*, *21*, 295–305, doi:10.1016/S0277-3791(01)00101-9.
- Wang, L., M. Sarnthein, P. M. Grootes, and H. Erlenkeuser (1999a), Millennial reoccurrence of century-scale abrupt events of East Asian monsoon: A possible heat conveyor for the global deglaciation, *Paleoceanography*, *14*(6), 725–731, doi:10.1029/1999PA900028.
- Wang, L., M. Sarnthein, H. Erlenkeuser, J. Grimalt, P. Grootes, S. Heilig, E. Ivanova, M. Kienast, C. Pelejero, and U. Pflaumann (1999b), East Asian monsoon climate during the late Pleistocene: High-resolution sediment records from the South China Sea, *Mar. Geol.*, *156*(1–4), 245–284, doi:10.1016/S0025-3227(98)00182-0.
- Wang, Y. J., H. Cheng, R. L. Edwards, Z. S. An, J. Y. Wu, C.-C. Shen, and J. A. Dorale (2001), A high-resolution absolute-dated late Pleistocene monsoon record from Hulu Cave, China, *Science*, *294*, 2345–2348, doi:10.1126/science.1064618.
- Wang, Y., H. Cheng, R. L. Edwards, Y. He, X. Kong, Z. An, J. Wu, M. J. Kelly, C. A. Dykoski, and X. Li (2005), The Holocene Asian monsoon: Links to solar changes and North Atlantic climate, *Science*, *308*, 854–857, doi:10.1126/science.1106296.
- Wang, Y., H. Cheng, R. L. Edwards, X. Kong, X. Shao, S. Chen, J. Wu, X. Jiang, X. Wang, and Z. An (2008), Millennial- and orbital-scale changes in the East Asian monsoon over the past 224,000 years, *Nature*, *451*, 1090–1093, doi:10.1038/nature06692.
- Xiang, R., Y. Sun, T. Li, D. W. Oppo, M. Chen, and F. Zheng (2007), Paleoenvironmental change in the middle Okinawa Trough since the last deglaciation: Evidence from the sedimentation rate and planktonic foraminiferal record, *Palaeogeogr. Palaeoclimatol. Palaeoecol.*, *243*, 378–393, doi:10.1016/j.palaeo.2006.08.016.
- Yokoyama, Y., K. Lambeck, P. De Deckker, P. Johnston, and L. K. Fifield (2000), Timing of the Last Glacial Maximum from observed sea-level minima, *Nature*, *406*, 713–716, doi:10.1038/35021035.
- Yokoyama, Y., T. M. Esat, and K. Lambeck (2001a), Coupled climate and sea-level changes deduced from Huon Peninsula coral terraces of the last ice age, *Earth Planet. Sci. Lett.*, *193*(3–4), 579–587, doi:10.1016/S0012-821X(01)00515-5.
- Yokoyama, Y., T. M. Esat, and K. Lambeck (2001b), Last glacial sea-level change deduced from uplifted coral terraces of Huon Peninsula, Papua New Guinea, *Quat. Int.*, *83–85*, 275–283, doi:10.1016/S1040-6182(01)00045-3.
- Yokoyama, Y., Y. Kido, R. Tada, I. Minami, R. C. Finkel, and H. Matsuzaki (2007), Japan Sea oxygen isotope stratigraphy and global sea-level changes for the last 50,000 years recorded in sediment cores from the Oki Ridge, *Palaeogeogr. Palaeoclimatol. Palaeoecol.*, *247*, 5–17, doi:10.1016/j.palaeo.2006.11.018.
- Yu, P.-S., C.-C. Huang, Y. Chin, H.-S. Mii, and M.-T. Chen (2006), Late Quaternary East Asian monsoon variability in the South China Sea: Evidence from planktonic foraminifera faunal and hydrographic gradient records, *Palaeogeogr. Palaeoclimatol. Palaeoecol.*, *236*, 74–90, doi:10.1016/j.palaeo.2005.11.038.
- Yuan, D., et al. (2004), Timing, duration, and transitions of the last interglacial Asian monsoon, *Science*, *304*, 575–578, doi:10.1126/science.1091220.
- Zhang, Q., C.-Y. Xu, T. Jiang, and Y. Wu (2007), Possible influence of ENSO on annual maximum streamflow of the Yangtze River, China, *J. Hydrol.*, *333*(2–4), 265–274, doi:10.1016/j.jhydrol.2006.08.010.
- Zhang, R., and T. L. Delworth (2005), Simulated tropical response to a substantial weakening of the Atlantic thermohaline circulation, *J. Clim.*, *18*, 1853–1860, doi:10.1175/JCLI3460.1.

Y.-P. Chang, Institute of Marine Geology and Chemistry, National Sun Yat-sen University, Kaohsiung 80424, Taiwan.

M.-T. Chen, Institute of Applied Geosciences, National Taiwan Ocean University, Keelung 20224, Taiwan. (mtchen@mail.ntou.edu.tw)

S.-J. Kao, Research Center for Environmental Changes, Academia Sinica, Taipei 11529, Taiwan.
H. Kawahata and Y. Yokoyama, Ocean Research Institute, University of Tokyo, 1-15-1 Minami-dai, Tokyo 164-8639, Japan.

H. Matsuzaki, Department of Nuclear Engineering and Management, University of Tokyo, Tokyo 113-8656, Japan.

W. G. Thompson, Department of Geology and Geophysics, Woods Hole Oceanographic Institution, Woods Hole, MA 02543, USA.